

# Vortex fluctuations in underdoped $\text{Bi}_2\text{Sr}_2\text{CaCu}_2\text{O}_{8+\delta}$ crystals

Sylvain Colson,<sup>1</sup> Marcin Konczykowski,<sup>1</sup> Marat B. Gaifullin,<sup>2</sup> Yuji Matsuda,<sup>2</sup> Piotr Gierlowski,<sup>3</sup> Ming Li,<sup>4</sup> Peter H. Kes<sup>4</sup> and Cornelis J. van der Beek<sup>1</sup>

<sup>1</sup>Laboratoire des Solides Irradiés, CNRS-UMR 7642 and CEA/DSM/DRECAM, Ecole Polytechnique, 91128 Palaiseau, France

<sup>2</sup>Institute for Solid State Physics, University of Tokyo, Kashiwanoha, Kashiwa, Chiba 277-8581, Japan

<sup>3</sup>Institute of Physics, Polish Academy of Sciences, Al. Lotnikow 32/46, 02-668 Warsaw, Poland

<sup>4</sup>Kamerlingh Onnes Laboratorium, Leiden University, P.O. Box 9506, 2300 RA Leiden, The Netherlands

(December 2, 2024)

Vortex thermal fluctuations in heavily underdoped  $\text{Bi}_2\text{Sr}_2\text{CaCu}_2\text{O}_{8+\delta}$  ( $T_c=69.4$  K) are studied using Josephson plasma resonance (JPR). From the data in zero magnetic field, we obtain the penetration depth along the  $c$ -axis,  $\lambda_{L,c}(0) = 229 \pm 10$   $\mu\text{m}$  and the anisotropy ratio  $\gamma(0) \approx 600$ . The low plasma frequency allows us to study phase correlations over the whole vortex solid (Bragg-glass) state. The JPR results yield a wandering length  $r_w$  of vortex pancakes. The temperature dependence of  $r_w$  as well as its increase with applied dc magnetic field can only be explained by the renormalization of the tilt modulus by thermal fluctuations, and suggest the latter is responsible for the dissociation of the vortices at the first order transition.

In the past years, Josephson plasma resonance (JPR) has proved to be a powerful tool in the study of vortex matter in layered superconductors [1–5]. A microwave electric field with polarization perpendicular to the superconducting layers gives rise to an interlayer Josephson current  $J_m^{(c)}$ . The magnitude of  $J_m^{(c)}$  can be measured through the Josephson plasma frequency  $\omega_{pl} \sim J_m^{(c)1/2}$ , at which the equality of charging and kinetic energy leads to a collective excitation of Cooper pairs across the layers. Because the plasma frequency is in the range 10-500 GHz, it is smaller than the superconducting gap ( $\approx 1$ -5 THz), so that plasma damping is unimportant [6]. Under applied magnetic field, the JPR frequency is given by [7]  $\omega_{pl}^2(B, T) = \omega_{pl}^2(0, T) \langle \cos(\phi_{n,n+1}) \rangle$ , where  $\phi_{n,n+1}$  is the gauge invariant phase difference between superconducting layer  $n$  and  $n+1$ , and  $\langle \dots \rangle$  stands for the thermal and disorder averaging. Thus, JPR is a probe of the interlayer phase coherence.

The fluctuations of pancake vortices created by a dc magnetic field applied perpendicular to the layers modify the relative phase difference between adjacent layers and thus depress the plasma frequency. Thermal fluctuations and disorder in the layers shift the pancakes with respect to their nearest neighbors in the  $c$  direction, by a distance  $\mathbf{r}_{n,n+1} = \mathbf{u}_{n+1} - \mathbf{u}_n$ . Here  $\mathbf{u}_n$  is the  $ab$ -plane displacement of the pancake vortex in layer  $n$  with respect to the equilibrium position of the stack it belongs to (Fig. 1). A wandering length of vortex lines, which is related directly to the JPR frequency  $\omega_{pl}^2$ , can be defined as  $r_w = \sqrt{\langle \mathbf{r}_{n,n+1}^2 \rangle}$  [8,9].

In this paper, we use JPR to study vortex fluctuations that lead to the first order transition (FOT) of vortex matter in the layered high- $T_c$  compound  $\text{Bi}_2\text{Sr}_2\text{CaCu}_2\text{O}_{8+\delta}$  (BSCCO). Vortex matter in BSCCO displays various phases with interesting features. At  $T \gtrsim 38$  K, the low-field ordered vortex Bragg glass [10]

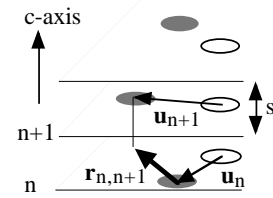


FIG. 1. Meandering of vortex pancakes along the vortex line in layered superconductors. Because of thermal fluctuations and disorder, pancakes (full circles) are shifted away from their equilibrium position (open circles).

undergoes a FOT into a high-temperature, high-field vortex liquid [11]. At  $T \lesssim 38$  K, the Bragg glass undergoes a transition towards a disordered vortex state with slow dynamics. Recently, Avraham *et al.* have observed inverse melting [12] of the vortex lattice at intermediate temperatures between 28 and 38 K. This means that, in this part of the phase diagram, the ordered vortex solid has a higher entropy than the disordered vortex phase. This was accounted for by important thermal fluctuations, yielding a larger entropy than can be gained through the disordering of the vortex lattice. It is the aim of this paper to quantify the thermal excursions of the pancake vortices which lead to the high entropy of the vortex solid.

Underdoped BSCCO ( $T_c=69.4$  K) single crystals were grown by the traveling solvent floating zone method in 25 mbar  $\text{O}_2$  partial pressure at the FOM-ALMOS center, the Netherlands [13]. The samples were post-annealed for one week at  $700^\circ\text{C}$  in flowing  $\text{N}_2$ . The advantage of using heavily underdoped BSCCO is that the JPR frequency in zero field and zero temperature turns out to be very low ( $\approx 61$  GHz), which allows us to measure  $\omega_{pl}$  and the vortex meandering over the entire vortex phase diagram. Samples A and B (cut from the same crystal) have dimensions  $1.35 \times 1 \times 0.04$   $\text{mm}^3$  and  $0.7 \times 0.47 \times 0.04$   $\text{mm}^3$ , respectively. Another sample from the same batch was

used to determine the temperature of the FOT. The JPR measurements were carried out using the cavity perturbation technique in the Laboratoire des Solides Irradiés (on sample A) and the bolometric method in the Institute for Solid State Physics at the University of Tokyo (on samples A and B). For the cavity perturbation technique, the sample was glued in the center of the top cover of a cylindrical Cu cavity used in the different  $\text{TM}_{01i}$  ( $i = 0, \dots, 4$ ) modes. These provide the correct configuration of microwave field at the sample location, in which  $E_{rf} \parallel c$ -axis and  $H_{rf} \approx 0$  [14]. The unloaded quality factor  $Q_0$  is measured as function of temperature and field to obtain the power absorbed by the sample (Fig. 2). The bolometric method [15] consists in measuring the heating of the sample induced by the absorption of the incident microwave power when the JPR is excited. Experimental details of this method have been described elsewhere [2,3,14].

Figure 3 shows the JPR frequency  $\omega_{pl}/2\pi$  in zero field obtained by the above-mentioned methods on samples A and B.  $\omega_{pl}^2$  is proportional to the maximum interlayer Josephson current along the  $c$ -axis [7],

$$\omega_{pl}^2(H, T) = \frac{2\pi\mu_0 c^2 s}{\epsilon_r \Phi_0} J_m^{(c)}(H, T) \quad (1)$$

where

$$J_m^{(c)}(H, T) = J_m^{(c)}(0, T) \langle \cos(\phi_{n,n+1}) \rangle \quad (2)$$

is the maximum Josephson current,  $s = 1.5$  nm is the interlayer spacing,  $\epsilon_r$  the high-frequency relative dielectric constant and  $\Phi_0$  the flux quantum. Using the Ambegaokar-Baratoff formula [16]  $J_m^{(c)}(0, T) = J_m^{(c)}(0, 0) \frac{\Delta(T)}{\Delta(0)} \tanh \frac{\Delta(T)}{2k_B T}$  as a phenomenological fit, and assuming a BCS-type variation of the superconducting gap [17]  $\Delta(T)$  with  $\Delta(0) = 2.1 k_B T_c$ , the temperature dependence of the JPR data in zero field for  $t < 0.8$  can be well described ( $t = T/T_c$  is the reduced temperature). The only parameter is the zero field, zero temperature plasma frequency  $\omega_{pl}(0, 0)/2\pi = 61.4$  GHz (see Fig. 3). Using  $\omega_{pl}(0, T) = c/\lambda_{L,c}(T)\sqrt{\epsilon_r}$  and  $\epsilon_r = 11.5$  [18], we obtain an estimate of the London penetration depth for currents along the  $c$ -axis at  $T=0$ ,  $\lambda_{L,c}(0) = 229 \pm 10$   $\mu\text{m}$ . Using the London in-plane penetration depth  $\lambda_{L,ab}(0) \approx 390$  nm obtained by reversible magnetization measurements on sample A, this corresponds to a  $\gamma(0) = \lambda_{L,c}(0)/\lambda_{L,ab}(0) \approx 600$ , which is consistent with other data [2,3] for the same material.

To analyze our JPR data in non-zero magnetic fields, we need a phenomenological fit to our experimental  $\omega_{pl}(0, T)$  data above  $t = 0.8$ . For this purpose, we have used the two-fluid model proposed by Kakeya *et al.* [19,20] which has  $\omega_{pl}^2(0, T) = \frac{1}{2}\omega_{pl}^2(0, 0)[1 - \tilde{\tau}^{-2} + \sqrt{(1 + \tilde{\tau}^{-2})^2 - 4\tilde{\tau}^{-2}t^4}]$  with  $\tilde{\tau} = \tau\omega_{pl}(0, 0)$  the reduced quasiparticle scattering rate. This model well describes

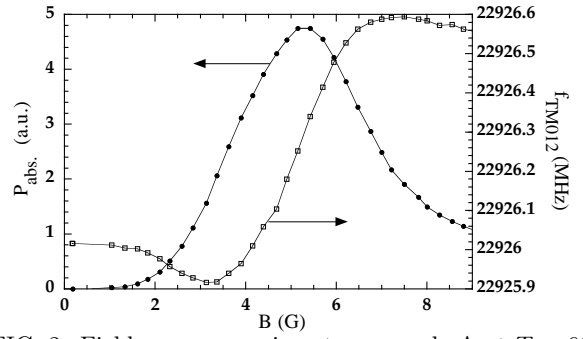


FIG. 2. Field sweep experiment on sample A at  $T = 66$  K in the  $\text{TM}_{012}$  mode of the cavity ( $f = 22.9$  GHz). The power absorbed (left) in the sample shows a maximum at  $B_{JPR} = 5.3$  G at which  $\omega = \omega_{pl}$ . At the same field, the resonance frequency of the cavity (right) displays a double-peak structure and a jump.

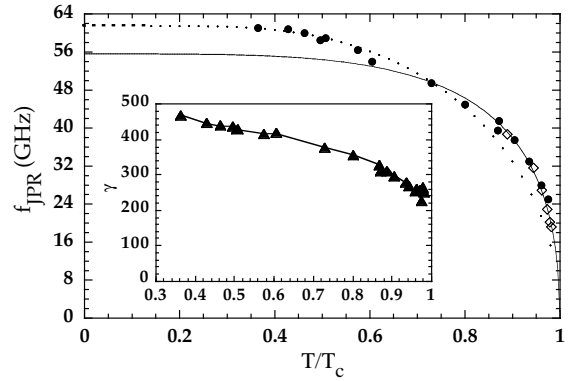


FIG. 3. The JPR frequency in zero magnetic field for samples A and B vs the reduced temperature  $T/T_c$ . The bolometric method (full circle) and the cavity perturbation technique (open diamond) have been used. Ambegaokar-Baratoff fit (dotted line) has been used to extract  $\omega_{JPR}(B=0, T=0)/2\pi = 61.4$  GHz, and a 2-fluid fit (solid line) was used when extracting the wandering length (see text). Inset : experimental temperature dependence of  $\gamma$ .

the data in the interval  $0.62 \leq t \leq 0.98$  if we choose  $\omega_{pl}(0, 0)/2\pi = 55.6$  GHz and  $\tau = 2 \times 10^{-12}$  s. Nevertheless, we point out that neither the Ambegaokar-Baratoff model nor the two-fluid model describes the experimental  $\omega_{pl}(0, T)$  data correctly in the whole temperature range.

From the results of  $\omega_{pl}(B, T)$ , we extract the vortex wandering length  $r_w$  in the following way. In the single vortex regime, at very low fields  $B < B_J, B_\lambda$ , Bulaevskii and Koshelev derived [8,9]

$$1 - \frac{\omega_{pl}^2(B, T)}{\omega_{pl}^2(0, T)} \approx \frac{\pi B}{2\Phi_0} r_w^2 \ln \frac{\lambda_J}{r_w} \quad (3)$$

where  $B_J = \Phi_0/\lambda_J^2$ ,  $B_\lambda = \Phi_0/4\pi\lambda_{ab}^2$  and the Josephson length  $\lambda_J = \gamma s$ . This relation is meaningful only for small excursions  $r_w \leq 0.6\lambda_J$ , i.e. for  $\langle \cos(\phi_{n,n+1}) \rangle = \omega_{pl}^2(B, T)/\omega_{pl}^2(0, T) \lesssim 1$ . More generally, one expects an increase of  $1 - \langle \cos(\phi_{n,n+1}) \rangle$  with  $r_w$  up

to a plateau for large  $r_w$ , as was found in recent simulations of the evolution of  $1 - \langle \cos(\phi_{n,n+1}) \rangle$  versus  $\langle u \rangle / a_0 \sim r_w / a_0$  for a pancake gas ( $a_0^2 = \Phi_0 / B$  is the intervortex spacing) [21]. The numerical data show that  $1 - \langle \cos(\phi_{n,n+1}) \rangle$  is almost quadratic in  $r_w$  for  $0 \lesssim 1 - \langle \cos(\phi_{n,n+1}) \rangle \lesssim 0.7-0.8$ , in agreement with Eq.(3) if the weak logarithmic dependence on  $\lambda_J / r_w$  is disregarded. Thus, we use

$$r_w^2 = \frac{2\Phi_0}{\pi B} (1 - \langle \cos(\phi_{n,n+1}) \rangle) \quad (4)$$

to obtain an approximation of the wandering length. Note that, because  $r_w = \sqrt{\langle (\mathbf{u}_{n+1} - \mathbf{u}_n)^2 \rangle} = \sqrt{2(u^2 - \langle \mathbf{u}_n \cdot \mathbf{u}_{n+1} \rangle)} \leq \sqrt{2}u$ ,  $r_w$  is a lower limit for the mean squared displacement of the vortex line  $u = \sqrt{\langle \mathbf{u}_n^2 \rangle}$ . In the case of completely uncorrelated layers (for a pancake gas for example), we have the equality  $r_w = \sqrt{2}u$ .

Figure 4 shows  $1 - \omega_{pl}^2(B, T) / \omega_{pl}^2(0, T) = 1 - \langle \cos(\phi_{n,n+1}) \rangle$  as function of temperature in nine different dc fields. The  $r_w$  vs  $t$  obtained by applying Eq.(4) is represented in Fig. 5. For every field, we observe an increase of  $r_w$  with  $T$  and, at constant temperature, we observe that  $r_w$  increases with the applied magnetic field indicating a field dependence of  $\omega_{pl}$  that deviates from the expected linear behavior (Eq.(3)). Another interesting feature of the  $r_w(T)$  curve is the break in the slope which appears at a field-dependent temperature and above which  $r_w$  has a field-independent behavior, i.e. all the curves merge into one described by the phenomenological fit  $r_w^0 / (1 - t)^{0.425}$ , with  $r_w^0 = 297$  nm. Alternatively, one may plot the same values of  $r_w$  vs  $T / T_{FOT}$ , where  $T_{FOT}$  is the FOT temperature (Fig. 5b). Here, two regimes appear clearly, delimited by  $0.96 T_{FOT}$ . For  $T < 0.96 T_{FOT}$ ,  $r_w$  increases roughly linearly, with a field-independent slope, whereas for  $T > 0.96 T_{FOT}$ , a stronger dependence of  $r_w$  is observed for lower fields.

We first discuss the temperature dependence of  $r_w$  at low fields. Using a simple evaluation of the elastic energy of a representative vortex in its lattice unit cell, we would expect  $u^2 \propto k_B T / \varepsilon_0 s$  with  $\varepsilon_0 = \Phi_0^2 / 4\pi\mu_0\lambda_{ab}^2$ , which is

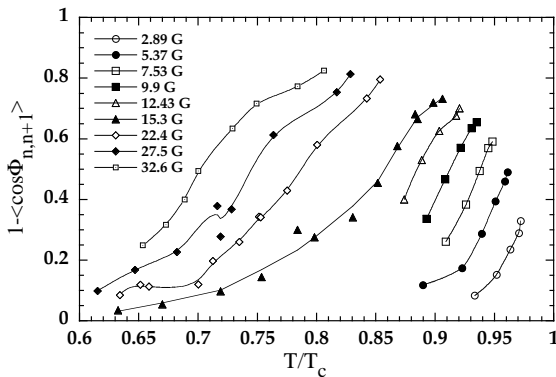


FIG. 4.  $1 - \langle \cos(\phi_{n,n+1}) \rangle$  vs temperature for different magnetic fields. We extract  $r_w$  from these data using Eq.(4).

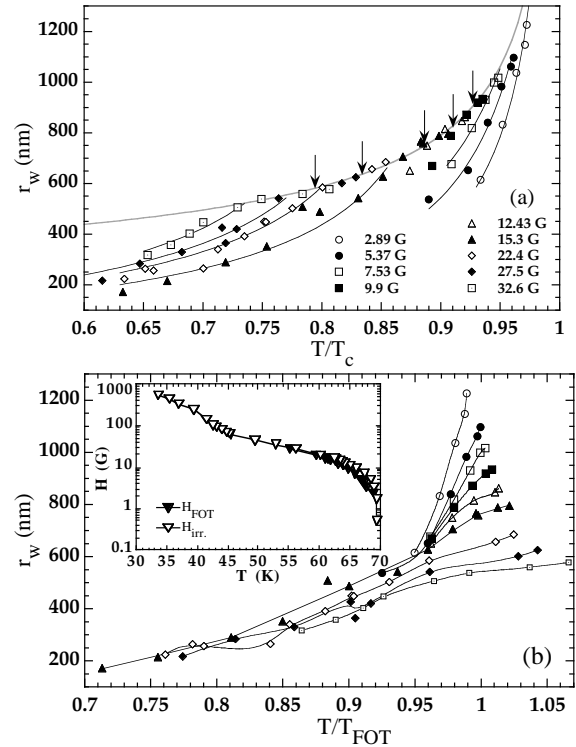


FIG. 5. (a) : Experimental  $r_w$  vs  $t = T/T_c$  under different magnetic fields in strongly underdoped BSCCO. For the fields 27.5, 22.4, 15.3, 12.43 and 9.9 G, vertical arrows show the temperature of the FOT. The grey line is a phenomenological fit  $r_w^0 / (1 - t)^{0.425}$ , with  $r_w^0 = 297$  nm. The other solid lines are fits to Eq.(6) with the single parameter  $\lambda_J = 415 \pm 17$  nm. (b) : The same  $r_w$  vs  $T/T_{FOT}$ . The solid lines are guide to the eye. Inset : phase diagram of a sample cut from the same crystal as samples A and B. Full and open triangles stands for the melting and the irreversibility fields, respectively.

inconsistent with our experimental results. More elaborate treatments were proposed by Dodgson *et al.* [22] who considered only electromagnetic coupling between pancakes, and by Koshchelev and Vinokur [23] and Goldin and Horowitz [24], who considered all contributions to the vortex lattice tilt modulus

$$c_{44}(\mathbf{k}) \approx \frac{B^2 / \mu_0}{1 + \lambda_c^2 k_{\parallel}^2 + \lambda_{ab}^2 Q_z^2} + \frac{\varepsilon_0}{2\gamma^2 a_0^2} \ln \left[ \frac{k_{max}^2}{K_0^2 + (Q_z / \gamma)^2} \right] + \frac{\varepsilon_0}{2\lambda_{ab}^2 Q_z^2 a_0^2} \ln \left( 1 + \frac{a_0^2}{21.3 r_w^2} \right). \quad (5)$$

Here,  $k_{\parallel} \approx \pi / r_w$  and  $Q_z \approx 2\gamma / a_0 \ll 2\pi / s$  are the wave vectors of the vortex line deformation parallel and perpendicular to the layers,  $k_{max} = \pi / r_w$  corresponds to the smallest possible deformation and  $K_0 = \sqrt{4\pi} / a_0$  [23,24]. All these parameters are known from our experimental results which allows us to directly compare  $r_w$  to theory. Writing  $U_{el} \approx c_{44} a_0^2 (u^2 / s) \approx k_B T$ , we obtain the approximate result

$$r_w^2 = \alpha u^2 \approx \alpha s \frac{k_B T}{c_{44} a_0^2}. \quad (6)$$

Figure 5a shows the good agreement between Eq.(6) and our  $r_w$  data in the Bragg-glass. For the lowest three fields, the three terms of  $c_{44}$  are used for the fit; for higher fields, a good fit is obtained if the nonlocal collective term (first term of  $c_{44}$ ) is omitted. If we set  $\alpha = 1$  and use the Ginzburg-Landau dependence  $\lambda_{ab}^2(t) = \lambda_{ab}^2(0)/(1-t)$ , all fits yield  $\lambda_J = 415 \pm 17$  nm. For the lowest fields and highest temperatures this agrees with our experimental value of  $\gamma$ , for higher fields it means  $r_w < u$  ( $r_w \approx 0.75u$  at  $t = 0.75$ ). We point out that in all cases, it is the softening of the line tension term of  $c_{44}$  by thermal fluctuations that correctly accounts for the field and the temperature dependence of our data.

Using the experimental values of  $r_w$ ,  $\lambda_{ab}$  and  $\gamma$ , we can also directly compare the relative strength of the three terms entering Eq.(5). Deep inside the Bragg-glass, the Josephson coupling (second term of  $c_{44}$ ) dominates over the magnetic coupling (third term of  $c_{44}$ ) and the nonlocal collective contribution. At very low fields, the Josephson coupling is predominant all the way to the FOT. Eq.(6) then reduces to Eq.(40) of ref. [24] with  $Q_z \approx 2\gamma/a_0$  instead of  $2\pi/s$ . At higher fields, the nonlocal collective contribution is expected to increase, becoming equal in magnitude to, and even larger than the Josephson term (line tension term) close to the FOT. In all cases, the magnetic term is irrelevant close to the FOT. Yet, our fits to Eq.(6) seem to suggest that the Josephson coupling term always dominates the tilt modulus of the vortex lattice near the FOT. This leads us to assert that the large thermal excursions of pancake vortices bring about the softening of the Josephson coupling contribution to  $c_{44}$  for the large-wavevector modes that lead to the FOT. Yet, for deformations with smaller wavevectors, the Josephson coupling still contributes to the line tension.

In conclusion, we have carried out JPR measurements on heavily underdoped BSCCO-2212 crystals using the cavity perturbation technique and the bolometric method. These data yield large values for the out-of-plane penetration depth ( $\lambda_{L,c}(0)=229 \pm 10\mu\text{m}$ ), the anisotropy parameter ( $\gamma(0)=\lambda_{L,c}(0)/\lambda_{L,ab}(0)\approx 600$ ) and the wandering length of vortex lines  $r_w$ . The observed temperature and field dependences of  $r_w$  are well accounted for by the renormalization of the Josephson term of the tilt modulus, i.e. the vortex line tension, by vortex thermal fluctuations. Our experimental data suggest that this renormalization eventually leads to the FOT.

We are grateful for financial support of the VORTEX program of the ESF (Europe Scientific Foundation) and NWO (Nederlandse Organisatie voor Wetenschappelijk Onderzoek). PG acknowledges support of Polish Government grant PBZ-KBN-013/T08/19.

- [1] O.K.C. Tsui, N.P. Ong, Y. Matsuda, Y.F. Yan, and J.B. Peterson, Phys. Rev. Lett. **73**, 724 (1994); Y. Matsuda, M.B. Gaifullin, and K. Kumagai, *ibid.* **75**, 4512 (1995); Y. Matsuda, M. B. Gaifullin, K. Kumagai, M. Kosugi and K. Hirata, *ibid.* **78**, 1972 (1997).
- [2] M.B. Gaifullin, Yuji Matsuda, N. Chikumoto, J. Shimoyama, K. Kishio, and R. Yoshizaki, Phys. Rev. Lett. **83**, 3928 (1999).
- [3] M.B. Gaifullin, Yuji Matsuda, N. Chikumoto, J. Shimoyama, and K. Kishio, Phys. Rev. Lett. **84**, 2945 (2000).
- [4] T. Shibauchi, T. Nakano, M. Sato, T. Kisu, N. Kameda, N. Okuda, S. Ooi, T. Tamegai, Phys. Rev. Lett. **83**, 1010 (1999).
- [5] K. Tamasaku, Y. Nakamura, S. Uchida, Phys. Rev. Lett. **69**, 1455 (1992); D. Dulic *et al.*, Phys. Rev. Lett. **86**, 4660 (2001).
- [6] M. Tachiki, T. Koyama, S. Takahashi, Phys. Rev. B **50**, 7065 (1994).
- [7] L. N. Bulaevskii, M. P. Maley, M. Tachiki, Phys. Rev. Lett. **74**, 801 (1995).
- [8] L.N. Bulaevskii, A. E. Koshelev, V. M. Vinokur, M. P. Maley, Phys. Rev. B **61**, R3819 (2000).
- [9] A. E. Koshelev and L. N. Bulaevskii, Physica C **341-348**, 1503 (2000).
- [10] T. Giamarchi and P. Le Doussal, Phys. Rev. B **55**, 6577 (1997).
- [11] R. Cubitt, E.M. Forgan, G. Yang, S.L. Lee, D. McK. Paul, H.A. Mook, M. Yethiraj, P.H. Kes, T.W. Li, A.A. Menovsky, Z. Tarnawski and K. Mortensen, Nature **365**, 410 (1993); E. Zeldov, D.Majer, M. Konczykowski, V.B. Geshkenbein, V.M. Vinokur, and H. Strikman, Nature **375**, 373 (1995).
- [12] N. Avraham, B. Khaykovich, Y. Myasoedov, M. Rappaport, H. Shtrikman, D. E. Feldman, T. Tamegai, P. H. Kes, Ming Li, M. Konczykowski, C. J. van der Beek, E. Zeldov Nature (London) **411**, 451 (2001)
- [13] Ming Li, to be published.
- [14] S. Colson, C. J. van der Beek, M. Konczykowski, M. B. Gaifullin, Y. Matsuda, P. Gierlowski, Ming Li, P. H. Kes, Physica C **369**, 236 (2002).
- [15] Y. Matsuda, N. P. Ong, Y. F. Yan, J. M. Harris, and J. B. Peterson, Phys. Rev. B **49**, 4380 (1994).
- [16] V. Ambegaokar and A. Baratoff, Phys. Rev. Lett. **10**, 486 (1963) & Errata, *ibid.* **11**, 104 (1963).
- [17] B. Mühlischlegel, Zeit. Phys. **155**, 313 (1959).
- [18] M.B. Gaifullin, Y. Matsuda, N. Chikumoto, J. Shimoyama, K. Kishio, R. Yoshizaki, Physica C **362**, 228 (2001).
- [19] K. Kadowaki, I. Kakeya, T. Wakabayashi, R. Nakamura, S. Takahashi, Int. J. Mod. Phys. B **14**, 547 (2000).
- [20] I. Kakeya, R. Nakamura, T. Wada, K. Kadowaki, Physica C **362**, 234 (2001).
- [21] E. H. Brandt and E. B. Sonin, preprint.
- [22] M. J. W. Dodgson, A. E. Koshelev, V. B. Geshkenbein and G. Blatter, Phys. Rev. Lett. **84**, 2698 (2000).
- [23] A. E. Koshelev, V. M. Vinokur, Phys. Rev. B **57**, 8026 (1998).
- [24] T. R. Goldin and B. Horovitz, Phys. Rev. B **58**, 9524 (1998).